NRC Research Press

ARTICLE

Geochemical characteristics and geological significance of the bedded chert during the Ordovician and Silurian transition in the Shizhu area, Chongqing, South China

Bin Lu, Zhen Qiu, Baohua Zhang, and Jian Li

Abstract: A large amount of bedded chert widely deposited during the Ordovician and Silurian transition in South China. In this study, analyses of the petrographic characteristics, the major elements and rare earth elements (REEs), were conducted on 31 bedded chert samples obtained from the Wufeng and Longmaxi Formations at the Qiliao section in the Shizhu area of the Sichuan Basin to determine the sedimentary environment and the origin of the bedded chert during the Ordovician and Silurian transition. The following conclusions were obtained: (*i*) the bedded chert in the Wufeng and Longmaxi Formations at the Qiliao Section originated mainly from terrigenous input and siliceous organisms and was slightly influenced by hydrothermal fluid, (*ii*) siliceous organisms were a key factor controlling the differences in the SiO_2 content of the bedded chert in the Wufeng and Longmaxi Formations at the Qiliao Section, and (*iii*) the bedded chert in the Wufeng and Longmaxi Formations deposited in a continental margin environment during the Ordovician and Silurian transition.

Key words: bedded chert, geochemistry, Wufeng Formation, Longmaxi Formation, shale gas, Sichuan Basin.

Résumé : Une importante quantité de chert lité a été déposée à grande échelle durant le passage Ordovicien-Silurien en Chine méridionale. Des analyses des caractéristiques pétrographiques, des éléments majeurs et des terres rares ont été réalisées sur 31 échantillons de chert lité des Formations de Wufeng et Longmaxi de la coupe de Qiliao de la région de Shizhu du bassin du Sichuan, afin de déterminer le milieu sédimentaire et l'origine des cherts lités durant le passage Ordovicien-Silurien. Les conclusions suivantes en sont tirées : (*i*) les cherts lités dans les Formations de Wufeng et Longmaxi de la coupe de Qiliao proviennent principalement d'apports terrigènes et d'organismes siliceux et ont subi une légère influence de fluides hydrothermaux, (*ii*) les organismes siliceux sont des facteurs clés expliquant les différences des teneurs en SiO_2 entre les Formations de Wufeng et de Longmaxi dans la coupe de Qiliao et (*iii*) les cherts lités des Formations de Wufeng et Longmaxi ont été déposés dans un milieu de marge continentale durant le passage Ordovicien-Silurien. [Traduit par la Rédaction]

Mots-clés : chert lité, géochimie, Formation de Wufeng, Formation de Longmaxi, gaz de schiste, bassin du Sichuan.

1. Introduction

Chert is predominantly composed of SiO_2 and is widely present throughout the geologic record. Numerous studies on chert have been carried out to reconstruct the evolution of paleoenvironment, paleogeography, and paleontology (Murray et al. 1990, 1991, 1992*a*, 1992*b*; Murray 1994; Xu 1996; Zhou et al. 2004; Chen et al. 2006; Du et al. 2006, 2007; Lin et al. 2010; Qiu and Wang 2010, 2011). Understanding the origin of chert is critical to reconstructing paleoenvironments. Oceanic silica is generally considered to be sourced from continental and submarine hydrothermal input and sinks with burial of siliceous organisms (diatom, radiolarian, and sponge) because of their radiation in the Phanerozoic Eon (Tréguer and De 2013). Therefore, the origin of the chert is closely related to contemporary oceanic silica cycling, which is further influenced by various other geological processes.

The bedded chert was widely distributed in the Wufeng and Longmaxi Formations during the Ordovician and Silurian transition in South China. The origin and sedimentary environment of the bedded chert in the Wufeng and Longmaxi Formations has received much less attention and remains controversial (Huang et al. 1991; Li 1997; Lei et al. 2002; Liu et al. 2010; Wang et al. 2014; Zhang et al. 2014; Ran et al. 2015; He et al. 2016). Researchers have argued that the bedded chert of Upper Ordovician and Lower Silurian in the Yangtze Block deposited under the influence of the interaction of volcanism and organisms in the deep water environment instead of the hydrothermal fluid environment (Huang et al. 1991; Ran et al. 2015). Others have suggested that the bedded chert in the Upper Ordovician and Lower Silurian in the Yangtze Block was derived from normal biochemical and chemical precipitation in the deep water (Li 1997; Lei et al 2002; Liu et al. 2010; Wang et al. 2014; Zou et al. 2018). Thus, the bedded chert in the

Received 27 June 2018. Accepted 17 November 2018.

Paper handled by Associate Editor Hao Deng.

B. Lu. Institute of Geochemistry, Chinese Academy of Sciences, Guiyang 550081, China; University of Chinese Academy of Sciences, Beijing 100049, China; PetroChina Research Institute of Petroleum Exploration and Development, Beijing 100083, China; National Energy Shale Gas Research & Development (Experiment) Center, Langfang 065007, China.
Z. Qiu. PetroChina Research Institute of Petroleum Exploration and Development, Beijing 100083, China; National Energy Shale Gas Research & Development (Experiment) Center, Langfang 065007, China.
B. Zhang. Institute of Geochemistry, Chinese Academy of Sciences, Guiyang 550081, China.
J. Li. PetroChina Research Institute of Petroleum Exploration and Development, Beijing 100083, China.
Corresponding authors: Zhen Qiu (email: qiuzhen316@163.com); Baohua Zhang (email: zhangbaohua@vip.gyig.ac.cn).

Fig. 1. (*a*) Paleogeographic map of the world (Torsvik and Cocks, 2013). (*b*) Paleogeographic map of the Sichuan Basin during the deposition of transition Wufeng Formation (modified from Zou et al. 2015). (*c*) Stratigraphic column and sample locations of the Qiliao section. [Colour online.]

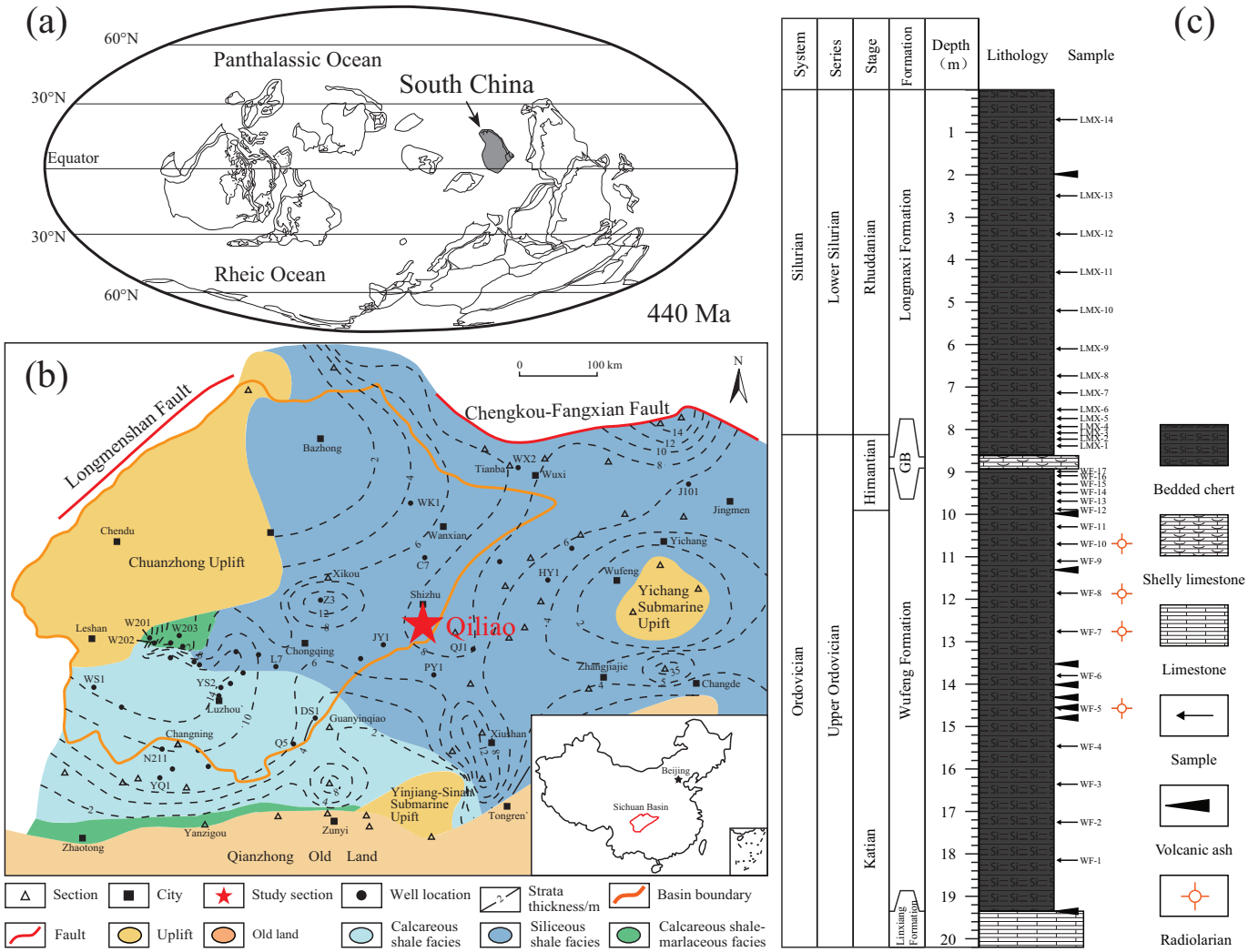

Wufeng and Longmaxi Formations in the Sichuan Basin may be derived from a complex origin and sedimentary environment. Basin, petrography, major elements, and rare earth elements (REEs) analyses were carried out to examine the origin and sedimentary environment of the bedded chert in the Wufeng and Longmaxi Formations in the Sichuan Basin. The Shizhu area, located in the eastern Sichuan Basin, was selected as a study area. The bedded chert in the Wufeng and Longmaxi Formations was generally rich in organic matter, which is of great significance in studying shale gas in the study area (Zou et al. 2010, 2015; Qiu et al. 2013, 2017).

2. Geological setting

The Sichuan Basin is located west of the Yangtze Block, south of Micang and Daba Mountains, east of Longmen Mountain, and north of Daliang and Lou Mountains (Wang et al. 2002; Dong et al. 2014). Since the Paleozoic era, the Sichuan Basin has experienced several stages of tectonic movement such as continuous tensioning, rifting, and thrusting (Su et al. 2007; Mou et al. 2011). During the Late Ordovician to the Early Silurian period, the Sichuan Basin was influenced by the collision of the Cathaysia Block and the Yangtze Block to form the Xuefeng uplift, Central Sichuan uplift, Central Guizhou uplift, and other paleo-uplift structures (Su et al. 2007; Mou et al. 2011; Yu et al. 2015). Therefore, the anoxic sedimentary environment was formed (Su et al. 2007; Mou et al. 2011). Influenced by marine transgression and tectonic movements, widespread graptolite-rich black shales with bedded chert were formed in the Wufeng Formation of the Upper Ordovician and the Longmaxi Formation of the Lower Silurian (Su et al. 2007, Zou et al 2015; Qiu et al. 2016, 2018).

The Qiliao section was located in the Shizhu area of Chongqing City, Sichuan Basin (Fig. 1). In ascending order, the Qiliao section can be divided into the Linxiang Formation, the Wufeng Formation, the Guanyinqiao Bed, and the Longmaxi Formation (Figs. 1–4). The Linxing Formation was dominated by limestone and marl, but the Wufeng and Longmaxi Formations consist of graptolite-rich black shales and bedded chert (Figs. 2*a* and 2*b*). Furthermore, a large volume of volcanic ash widely deposited within the strata of the Wufeng and Longmaxi Formations. The glaciation in Gondwana resulted in the rapid sea level fall at the end of the Ordovician, and the Guanyinqiao Bed shelly limestones (about 30 cm thick) were deposited and recorded with fossils of Hirnantia fauna (Rong 1984).

3. Samples and methods

We collected 31 well-preserved samples of the bedded chert were collected; 17 samples came from the Wufeng Formation and 14 samples from the Longmaxi Formation of the Qiliao section in

Fig. 2. Outcrop photos and microscopic features of the bedded chert at the Qiliao section. (*a*) Outcrop photo of the Qiliao section, (*b*) outcrop photo of the bedded chert in the Wufeng Formation, (*c*) radiolarian fossils in WF-5, (*d*) radiolarian fossils in WF-7, (*e*) radiolarian fossils in WF-8, and (*f*) radiolarian fossils in WF-10). [Colour online.]

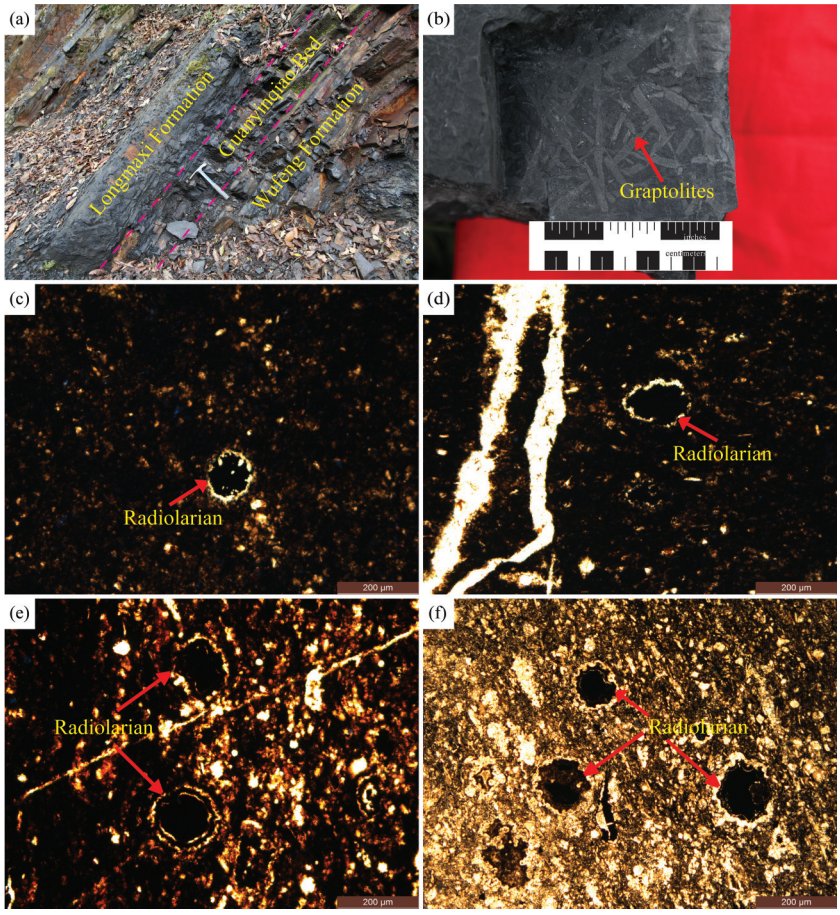

the Shizhu area of Chongqing (Figs. 3 and 4). Petrological observation and geochemical analyses were carried out. The petrological observation was mainly based on outcrop description and thin section observation. Geochemical analyses of major elements and REEs were completed at the Institute of Geology and Geophysics, Chinese Academy of Sciences. The major elements were tested using AXIOS Minerals made by PANalytical Corporation of Holland, and analytical precision for major element concentrations was generally better than 1%. REEs were tested using element inductively coupled plasma mass spectrometry (ICP-MS) from FINNIGAN MAT Company, and the analytical precision for REE concentrations was generally better than 3%. Normalization values for REEs were a mean of North American, European, and Russian shale composites (Sholkovitz, 1988). Ce anomaly (δCe) and Eu anomaly (δEu) were calculated using equations $\delta Ce = 2Ce_n/(La_n + Pr_n)$ and $\delta Eu = Eu_n/(Sm_n{}^*Gd_n)^{1/2}$, respectively, where *n* represents the average shale standardization.

4. Results

4.1. Petrological characteristics

At the Qiliao Section, the bedded chert in the Wufeng and Longmaxi Formations is unweathered, grey-black in color, rich in graptolite, and is characterized by high hardness and great brittleness (Figs. 2*a* and 2*b*). Volcanic ash layers in the Wufeng Formation were distributed at multiple intervals, whereas those in the Longmaxi Formation were comparatively fewer. Thin section observations indicated that some of the samples from the Wufeng and Longmaxi Formations contained a small amount of siliceous organisms such as radiolarians and sponge spicules (Figs. 2–4). Radiolarians made up less than 5% of the total sample, and they have a rounded or oval shape with a diameter of 50–150 μm.

4.2. Geochemical characteristics

4.2.1. Major elements

Analytical results of the major elements in the bedded chert in the Wufeng and Longmaxi Formations are listed in Table 1, showing some differences in content. Comparatively, the bedded chert in the Wufeng Formation had higher SiO_2 content ranging from 64.7% to 90.2% (average 82.92%), low TiO_2 content ranging from 0.15% to 0.62% (average 0.33%), and low Al_2O_3 content ranging from 3.22% to 12.31% (average 6.39%). However, the bedded chert in the Longmaxi Formation had low SiO_2 content ranging from 66.64% to 80.7% (average 74.51%), high TiO_2 content ranging from 0.34% to 0.73% (average 0.53%), and high Al_2O_3 content ranging from 6.36% to 13.21% (average 9.59%). The total Fe_2O_3 content (TFe_2O_3) in the bedded chert in the Wufeng Formation was close to that of the Longmaxi Formation with the TFe_2O_3 from 0.58% to 4.92% (average 1.61%) and from 1.11% to 3.52% (average 2.03%) in the Wufeng and Longmaxi Formations, respectively.

In addition, the ratios of Fe/Ti in the bedded chert in the Wufeng Formation (2.5–11.91, average 5.86) were higher than that of the Longmaxi Formation (1.78–6.76, average 4.88). However, the ratios of Al/(Al + Fe + Mn) in the bedded chert in the Wufeng Formation (0.59–0.89, average 0.76) were close to that of the Longmaxi Formation (0.71–0.9, average 0.77). The ratios of $Al_2O_3/(Al_2O_3 + TFe_2O_3)$ in the bedded chert in the Wufeng Formation

Fig. 3. The distribution of total organic carbon (TOC) and major elements of bedded chert in the Wufeng (WF) and Longmaxi (LMX) Formations at the Qiliao section. [Colour online.]

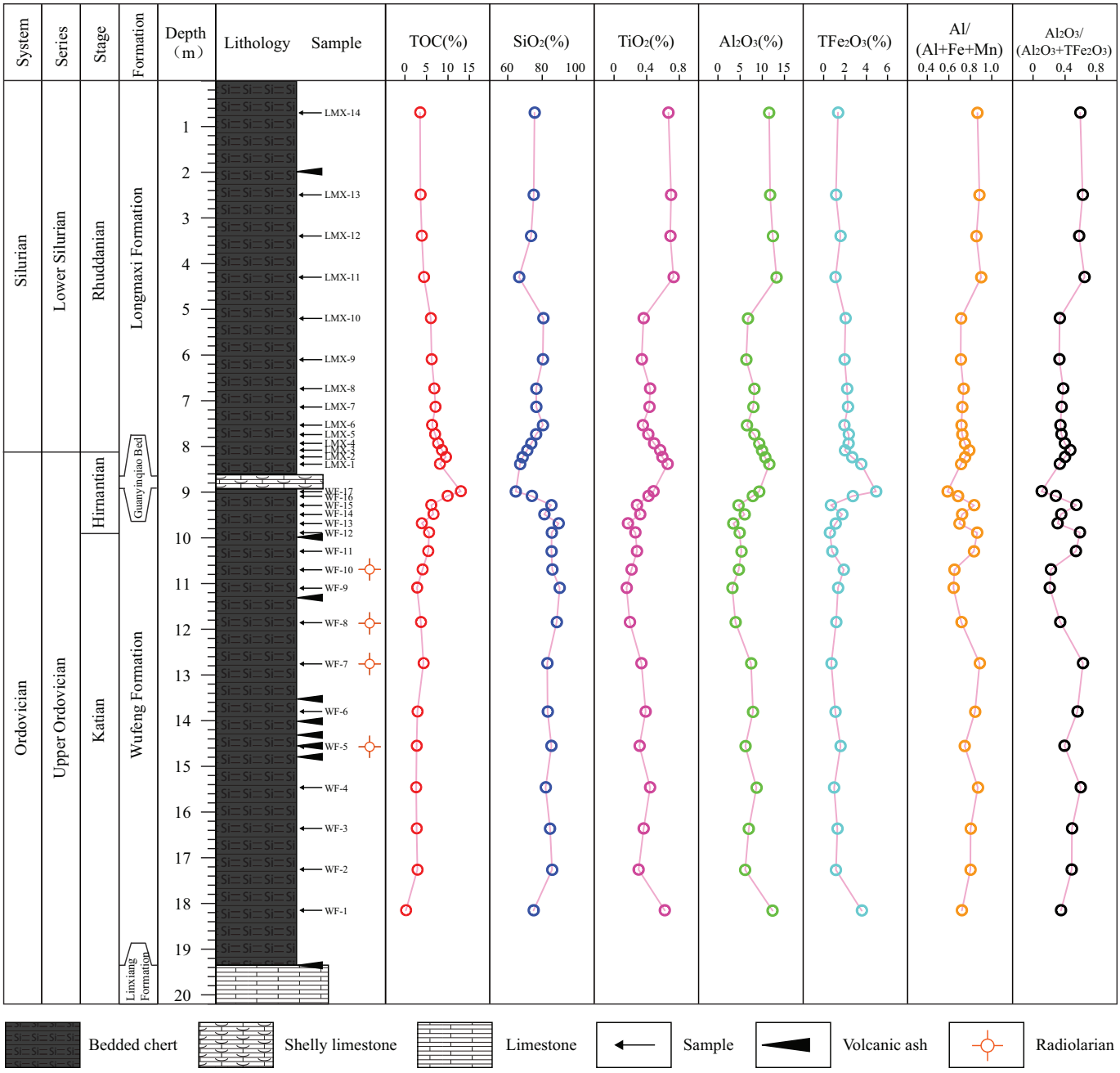

(0.65–0.91, average 0.81) were also close to that of the Longmaxi Formation (0.76–0.92, average 0.82). However, the ratios of TFe_2O_3/TiO_2 in the bedded chert in the Wufeng Formation (2.15–10.21, average 5.02) were higher than that of the Longmaxi Formation (1.52–5.79, average 4.18).

4.2.2. Rare Earth Elements (REEs)

Analytical results of REEs in the bedded chert, which also show differences in content between the Wufeng and Longmaxi Formations, are listed in Table 2. Total REE abundances (∑REE) of the bedded chert in the Wufeng Formation (66.57–240.31 parts per million (ppm), average 125.91 ppm) were lower than that of the Longmaxi Formation (141.43–322.92 ppm, average 189.43 ppm). The bedded chert in the Wufeng Formation showed a slightly negative Ce anomaly (0.91–1.08, average 0.96), whereas no Ce anomaly was found in the Longmaxi Formation (0.95–1.03, average 0.99). All samples in the Wufeng Formation (0.72–0.95, average 0.84) and the Longmaxi Formation (0.78–0.91, average 0.83) showed notable negative Eu anomaly. Moreover, the ratios of $(La/Yb)_n$ in the bedded chert in the Wufeng Formation (0.78–2.23, average 1.23) were slightly lower than those in the Longmaxi Formation (1.03–2.41, average 1.43), but the ratios of $(La/Ce)_n$ in the bedded chert in the Wufeng Formation (0.96–1.25, average 1.11) were close to those of the Longmaxi Formation (0.97–1.09, average 1.03).

5. Discussion

5.1. Origin of the bedded chert

Many studies on the origin of chert suggested that its origin was biogenic, metasomatic, and biochemical (Adachi et al. 1986; Yu

Fig. 4. The distribution of total organic carbon (TOC) and rare earth elements of bedded chert in the Wufeng (WF) and Longmaxi (LMX) Formations at the Qiliao section. [Colour online.]

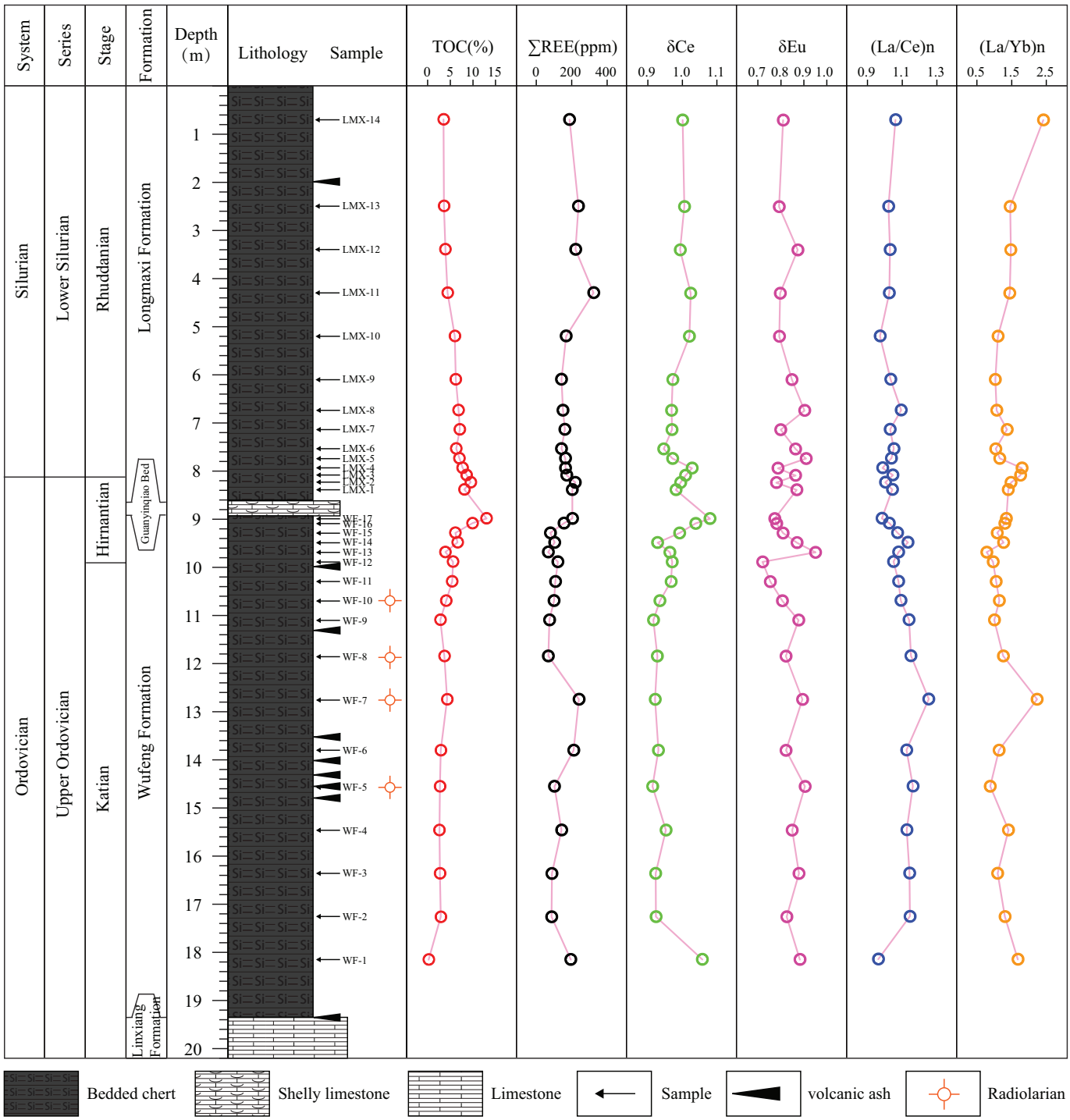

et al. 2004; Ma et al. 2011; Qiu and Wang 2010, 2011). Some studies indicated that the chert in the Precambrian strata was related to the submarine hydrothermal fluid (Zhou et al. 1994; Simonson et al. 2005; Chen et al. 2009). Furthermore, Paleozoic chert might originate from the accumulation of biogenic silica or the deposition of dissolved biogenic silica (Thurston 1972; Murchey and Jones 1992; Kametaka et al. 2005). However, chert originated from the submarine hydrothermal fluid during the Paleozoic era was also reported in other studies (Yamamoto 1987; Zhou 1990; Qiu and Wang 2010, 2011).

5.1.1. Sources of silica: terrigenous input and siliceous organisms

Major elements, including Mn, Fe, Al, Ti, and REEs, are hardly influenced by digenesis and are thus effective geochemical indicators to distinguish the chert of hydrothermal origin from biogenic origin (Murray 1994). Fe and Mn in chert were important indicators of hydrothermal fluid, and Al and Ti were related to terrigenous input (Boström and Peterson 1969; Adachi et al. 1986; Yamamoto 1987; Murray 1994). Adachi et al. (1986) established the Al–Fe–Mn ternary diagram for distinguishing the origin of silica. Their diagram shows that the chert without hydrothermal

Table 1. Major element compositions (%) of the bedded chert in the Wufeng (WF) and Longmaxi (LMX) Formations at the Qiliao section.

Sample	SiO_2	TiO_2	Al_2O_3	TFe_2O_3	MnO	Fe/Ti	Al/(Al + Fe + Mn)	TFe_2O_3/TiO_2	Al_2O_3/(Al_2O_3 + TFe_2O_3)	SiO_2/Al_2O_3	Al_2O_3/TiO_2
WF-1	75.04	0.62	12.31	3.58	0.01	6.72	0.72	5.76	0.77	6.10	19.81
WF-2	85.81	0.30	6.11	1.15	0.00	4.47	0.80	3.83	0.84	14.04	20.35
WF-3	84.60	0.36	6.94	1.29	0.00	4.15	0.80	3.56	0.84	12.19	19.14
WF-4	82.08	0.44	8.68	0.98	0.00	2.59	0.87	2.22	0.90	9.46	19.70
WF-5	85.42	0.31	6.18	1.58	0.00	5.91	0.75	5.06	0.80	13.82	19.81
WF-6	83.23	0.39	7.89	1.10	0.00	3.32	0.84	2.84	0.88	10.55	20.39
WF-7	83.03	0.34	7.45	0.72	0.00	2.50	0.89	2.15	0.91	11.14	22.21
WF-8	88.51	0.19	3.94	1.18	0.00	7.13	0.72	6.11	0.77	22.46	20.39
WF-9	90.20	0.15	3.22	1.35	0.00	10.21	0.64	8.75	0.70	28.01	20.87
WF-10	85.90	0.21	4.67	1.89	0.00	10.30	0.65	8.83	0.71	18.39	21.81
WF-11	85.44	0.28	5.26	0.80	0.00	3.32	0.83	2.85	0.87	16.24	18.73
WF-12	85.58	0.26	4.86	0.58	0.00	2.59	0.86	2.22	0.89	17.61	18.63
WF-13	89.59	0.17	3.42	1.12	0.00	7.73	0.70	6.62	0.75	26.20	20.22
WF-14	81.27	0.32	6.00	1.74	0.00	6.34	0.72	5.44	0.78	13.55	18.74
WF-15	85.34	0.28	4.58	0.68	0.00	2.83	0.84	2.43	0.87	18.63	16.35
WF-16	73.96	0.42	7.82	2.73	0.00	7.59	0.68	6.51	0.74	9.46	18.64
WF-17	64.70	0.48	9.28	4.92	0.01	11.91	0.59	10.21	0.65	6.97	19.25
LMX-1	67.20	0.65	11.57	3.52	0.01	6.27	0.71	5.38	0.77	5.81	17.67
LMX-2	68.69	0.59	10.64	2.67	0.01	5.27	0.75	4.52	0.80	6.46	18.01
LMX-3	71.30	0.56	9.91	1.99	0.01	4.12	0.79	3.53	0.83	7.19	17.57
LMX-4	73.70	0.49	9.29	2.34	0.01	5.56	0.75	4.77	0.80	7.93	18.93
LMX-5	76.52	0.42	8.19	2.35	0.01	6.55	0.72	5.61	0.78	9.34	19.57
LMX-6	80.46	0.35	6.53	1.94	0.01	6.45	0.72	5.53	0.77	12.32	18.61
LMX-7	76.62	0.43	7.95	2.27	0.01	6.13	0.72	5.25	0.78	9.64	18.40
LMX-8	76.59	0.44	8.21	2.20	0.01	5.82	0.74	4.99	0.79	9.33	18.61
LMX-9	80.45	0.34	6.36	1.96	0.00	6.76	0.71	5.79	0.76	12.65	18.79
LMX-10	80.70	0.36	6.74	2.05	0.00	6.64	0.71	5.69	0.77	11.97	18.71
LMX-11	66.64	0.73	13.21	1.11	0.00	1.78	0.90	1.52	0.92	5.04	18.14
LMX-12	73.56	0.69	12.38	1.57	0.00	2.66	0.86	2.28	0.89	5.94	17.97
LMX-13	75.09	0.70	11.76	1.16	0.00	1.94	0.88	1.67	0.91	6.39	16.88
LMX-14	75.60	0.67	11.53	1.35	0.00	2.37	0.87	2.03	0.90	6.56	17.32

Note: Some data are from Zou et al. 2018.

Table 2. REEs compositions (ppm) of the chert in the Wufeng (WF) and Longmaxi (LMX) Formations at the Qiliao section.

Sample	La	Ce	Pr	Nd	Sm	Eu	Gd	Tb	Dy	Ho	Er	Tm	Yb	Lu	∑REE	δCe	δEu	$(La/Yb)_n$	$(La/Ce)_n$
WF-1	42.21	88.72	10.02	33.96	5.12	0.90	3.72	0.63	3.51	0.68	2.10	0.32	2.15	0.34	194.36	1.06	0.88	1.68	0.96
WF-2	20.28	35.85	4.46	15.09	2.38	0.41	1.94	0.31	1.73	0.36	1.18	0.19	1.33	0.22	85.72	0.92	0.83	1.31	1.14
WF-3	20.08	35.58	4.44	16.49	2.56	0.46	1.94	0.32	1.93	0.39	1.29	0.22	1.56	0.26	87.52	0.92	0.88	1.10	1.14
WF-4	33.97	61.06	7.24	24.62	3.63	0.64	2.87	0.47	2.74	0.59	1.92	0.31	2.06	0.33	142.43	0.95	0.85	1.41	1.13
WF-5	23.63	41.16	5.15	17.39	2.77	0.56	2.58	0.44	2.70	0.61	1.94	0.30	2.29	0.36	101.88	0.91	0.90	0.88	1.16
WF-6	46.78	84.16	10.49	38.23	6.31	1.15	5.68	1.02	6.91	1.27	3.83	0.55	3.52	0.53	210.43	0.93	0.82	1.14	1.13
WF-7	64.00	103.42	11.57	41.48	5.50	0.95	3.75	0.56	3.09	0.67	2.15	0.33	2.45	0.38	240.31	0.92	0.89	2.23	1.25
WF-8	15.01	26.41	3.23	12.69	2.32	0.43	2.20	0.34	1.92	0.39	1.08	0.17	1.02	0.16	67.38	0.93	0.82	1.26	1.15
WF-9	15.21	27.03	3.44	13.98	2.96	0.66	3.55	0.54	2.92	0.56	1.47	0.23	1.30	0.21	74.05	0.92	0.88	1.00	1.14
WF-10	20.94	38.80	4.95	19.32	3.41	0.64	3.44	0.55	3.05	0.62	1.81	0.25	1.56	0.24	99.57	0.93	0.81	1.15	1.09
WF-11	23.08	43.31	5.21	20.13	3.32	0.58	3.28	0.54	3.21	0.66	2.00	0.30	1.87	0.28	107.78	0.97	0.75	1.06	1.08
WF-12	24.93	48.06	5.91	23.22	4.03	0.67	3.93	0.66	3.89	0.80	2.41	0.35	2.21	0.34	121.4	0.97	0.72	0.97	1.05
WF-13	13.88	26.03	3.16	12.49	2.25	0.48	2.08	0.36	2.09	0.44	1.34	0.21	1.52	0.23	66.57	0.96	0.95	0.78	1.08
WF-14	23.75	42.44	5.28	17.95	3.14	0.59	2.71	0.46	2.75	0.58	1.66	0.25	1.60	0.24	103.39	0.93	0.87	1.27	1.13
WF-15	17.39	32.82	3.77	14.37	2.15	0.39	2.03	0.34	2.11	0.46	1.44	0.21	1.37	0.21	79.07	0.99	0.81	1.09	1.07
WF-16	33.55	66.23	7.26	27.38	4.50	0.82	4.53	0.68	4.21	0.81	2.31	0.38	2.20	0.35	155.21	1.04	0.78	1.30	1.03
WF-17	42.61	87.70	9.27	36.31	6.20	1.10	5.96	0.93	5.63	1.11	3.05	0.48	2.70	0.42	203.45	1.08	0.77	1.35	0.98
LMX-1	43.49	84.36	10.21	38.22	6.29	1.19	5.43	0.91	5.15	0.97	2.86	0.43	2.65	0.39	202.56	0.98	0.87	1.40	1.04
LMX-2	45.58	91.94	11.27	41.87	6.93	1.22	6.46	0.99	5.53	1.08	3.16	0.43	2.63	0.39	219.48	0.99	0.78	1.48	1.00
LMX-3	38.00	73.53	8.37	31.98	4.78	0.89	4.09	0.66	3.69	0.73	2.06	0.28	1.85	0.27	171.18	1.01	0.86	1.75	1.05
LMX-4	34.03	69.76	8.13	31.22	5.54	0.98	5.13	0.72	3.98	0.74	1.90	0.29	1.62	0.25	164.29	1.03	0.79	1.80	0.99
LMX-5	32.63	63.64	7.91	32.91	6.25	1.29	5.93	0.95	5.44	0.95	2.68	0.39	2.41	0.35	163.73	0.97	0.91	1.16	1.04
LMX-6	28.40	54.65	7.07	26.91	5.42	1.16	6.08	0.84	4.60	0.88	2.43	0.33	2.33	0.34	141.43	0.95	0.86	1.04	1.05
LMX-7	32.98	64.76	8.13	31.04	5.68	1.04	5.53	0.82	4.65	0.86	2.31	0.37	2.06	0.32	160.54	0.97	0.80	1.37	1.03
LMX-8	31.48	58.24	6.88	29.69	5.11	1.12	5.50	0.80	4.38	0.94	2.65	0.36	2.52	0.37	150.05	0.97	0.90	1.07	1.09
LMX-9	27.92	54.69	6.82	28.15	5.38	1.08	5.52	0.85	4.58	0.90	2.58	0.37	2.32	0.36	141.52	0.97	0.85	1.03	1.03
LMX-10	32.50	67.62	8.13	33.02	6.25	1.16	6.29	0.93	5.08	0.96	2.88	0.39	2.51	0.38	168.09	1.02	0.79	1.11	0.97
LMX-11	70.19	138.51	15.63	56.37	9.91	1.74	8.87	1.35	8.42	1.64	4.83	0.67	4.16	0.61	322.92	1.02	0.80	1.45	1.03
LMX-12	46.80	91.98	11.00	41.83	7.35	1.41	6.52	1.06	5.98	1.06	3.01	0.44	2.71	0.40	221.56	0.99	0.87	1.48	1.03
LMX-13	51.07	101.19	11.91	43.81	7.33	1.25	6.25	0.98	5.61	1.08	3.28	0.46	3.00	0.46	237.68	1.01	0.79	1.46	1.02
LMX-14	43.62	83.16	9.48	33.42	4.95	0.80	3.66	0.55	3.03	0.59	1.67	0.27	1.55	0.24	187.00	1.00	0.81	2.41	1.06

influence is rich in Al, whereas hydrothermal chert is rich in Fe. Boström and Peterson (1969) proposed that the ratio of Al/(Al + Fe + Mn) was a good indicator of hydrothermal origin, which would increase with the distance away from the center of expansion. Boström et al. (1973) reported that the ratio of Al/(Al + Fe + Mn) in the chert related to hydrothermal fluid was smaller than 0.4, and that related to terrigenous input was higher than 0.4. In addition, Adachi et al. (1986) and Yamamoto (1987) reported that the ratio of Al/(Al + Fe + Mn) in pure chert related to hydrothermal fluid is 0.01, whereas that related to siliceous organisms is 0.6. By studying marine sediments, Boström et al. (1973) grouped chert found in present marine sediments based on biological, hydrothermal, and terrigenous origin, and established the Fe/Ti-Al/(Al + Fe + Mn) relationship diagram. Sugisaki et al. (1982) reported that the ratio of Al_2O_3/TiO_2 of the chert in normal marine sedimentary is 22.08 ± 2.32, but that of Al_2O_3/TiO_2 and Al/(Al + Fe + Mn) is significantly lowered when mixed with volcanic debris (Yamamoto et al. 1997). Huang et al. (2012*a*, 2013) suggested that the ratio of Al_2O_3/TiO_2, which is an important geochemical indicator of the chert origin, is only slightly influenced by deposition, digenesis, and weathering, and they established the relationship diagrams of Al_2O_3/TiO_2-Al/(Al + Fe + Mn) and Al_2O_3-SiO_2/Al_2O_3.

In our study, the relationship diagrams among SiO_2, TiO_2, Al_2O_3, and TFe_2O_3 indicate a strong negative correlation between the SiO_2 content with TiO_2 and Al_2O_3 in samples from the Wufeng and Longmaxi Formations, but a poor correlation with TFe_2O_3 (Fig. 5). Therefore, all the bedded chert in the Wufeng and Longmaxi Formations were interpreted related to terrigenous input and were slightly influenced by hydrothermal fluid. Excessive biogenic silica should be responsible for the strong negative correlation between SiO_2 and TiO_2 or Al_2O_3 (Fig. 5). Excessive silica with average content above ca. 20% would also dilute other elements such as TiO_2 and Al_2O_3. Based on the lower contents of TiO_2 and Al_2O_3 in the Wufeng Formation compared with the Longmaxi Formation as shown in Fig. 5, most samples from the Wufeng Formation have a higher content of excessive silica than those of the Longmaxi Formation (see Section 5.1.2.), suggesting a higher dilution effect for the samples in the Wufeng Formation.

Furthermore, based on the Al–Fe–Mn ternary diagram (Fig. 6*a*), all the samples from the Wufeng and Longmaxi Formations were plotted in the nonhydrothermal chert field (Fig. 6*a*). Thus, the bedded chert from both the Wufeng and Longmaxi Formations were slightly influenced by hydrothermal fluid. The ratios of Al/(Al + Fe + Mn) of the bedded chert in the Wufeng Formation varied from 0.59 to 0.89 (average 0.76) and ranged from 0.71 to 0.9 (average 0.77) in the Longmaxi Formation. The ratios of Al/(Al + Fe + Mn) in samples from the Wufeng and Longmaxi Formations were higher than those of pure chert (0.6), indicating that the siliceous source was dominated by terrigenous input and siliceous organisms. In Fe/Ti–Al/(Al + Fe + Mn) diagram, the distribution of samples from both the Wufeng and Longmaxi Formations was similar. Most samples were plotted near the terrigenous sediments and biogenic chert field, and only one sample in the Wufeng Formation was plotted in the average offshore clay field (Fig. 6*b*). Therefore, the origin of the bedded chert in the study area was mainly related to terrestrial input and organism. The Al_2O_3–SiO_2/Al_2O_3 diagram showed that the "pure chert" content of all samples from the Wufeng and Longmaxi Formations was low and mainly ranged from 50% to 85% and 30% to 65%, respectively (Fig. 6*c*), indicating that the bedded chert in the Wufeng and Longmaxi Formations was mainly influenced by terrigenous input and organisms, with more organisms influencing chert found in the Wufeng Formation compared with the Longmaxi Formation. The relationship between Al_2O_3/TiO_2 and Al/(Al + Fe + Mn) also revealed that the bedded chert in the Wufeng and Longmaxi Formations was nonhydrothermal and was associated with normal marine deposits (Fig. 6*d*).

Fig. 5. Relationship diagrams between SiO_2 and TiO_2, Al_2O_3, and TFe_2O_3 of bedded chert in the Wufeng and Longmaxi Formations at the Qiliao section. [Colour online.]

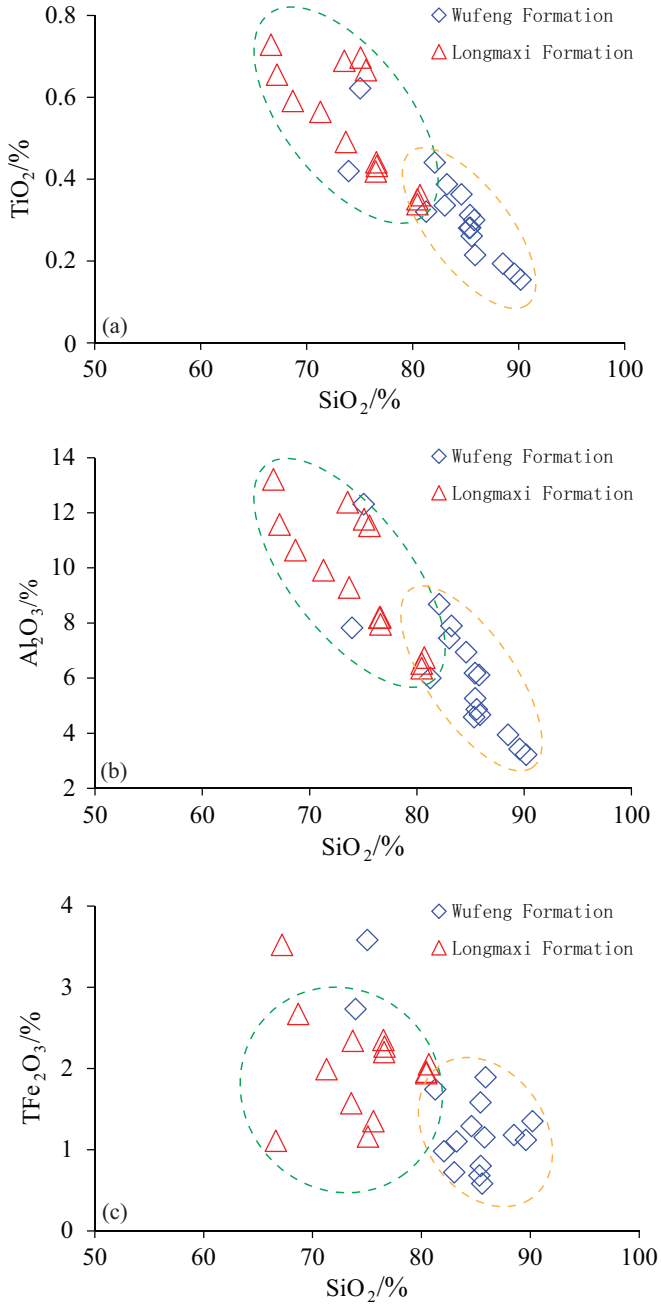

REEs are usually used as significant indicator for studying the origin of chert, especially for identifying hydrothermal chert (Michard 1989; Zhou et al. 2004; Chen et al. 2006; Qiu and Wang 2010, 2011). Murray et al. (1990, 1991) proposed that the two main REE sources in the marine sedimentary environment are derived from seawater and from terrigenous materials or volcanic particles. ∑REE in seawater was low and showed a slight negative Ce anomaly under the anoxic condition (Bolhar et al. 2004). Based on previous studies, the chert deposited close to the hydrothermal vent is characterized by a notable positive Eu anomaly, and increasing negative Ce anomaly is related to increasing distance away from the hydrothermal vent (Douville et al. 1999; Dias et al. 2011). The chert influenced by terrigenous input shows high ∑REE and enrichment of light REEs without notable Ce anomaly

Fig. 6. Relationship diagrams of chert origin in the Wufeng and Longmaxi Formations at the Qiliao section. (*a*) Hydrothermal chert associated with the basaltic volcanism (after Adachi et al. 1986), (*b*) nonhydrothermal chert containing felsic vocanic clasts (after Boström et al. 1973), (*c*) nonhydrothermal chert associated with the normal marin deposits (after Huang et al. 2013), and (*d*) nonhydrothermal chert containing basaltic vocanic clasts (after Huang et al. 2012*a*). [Colour online.]

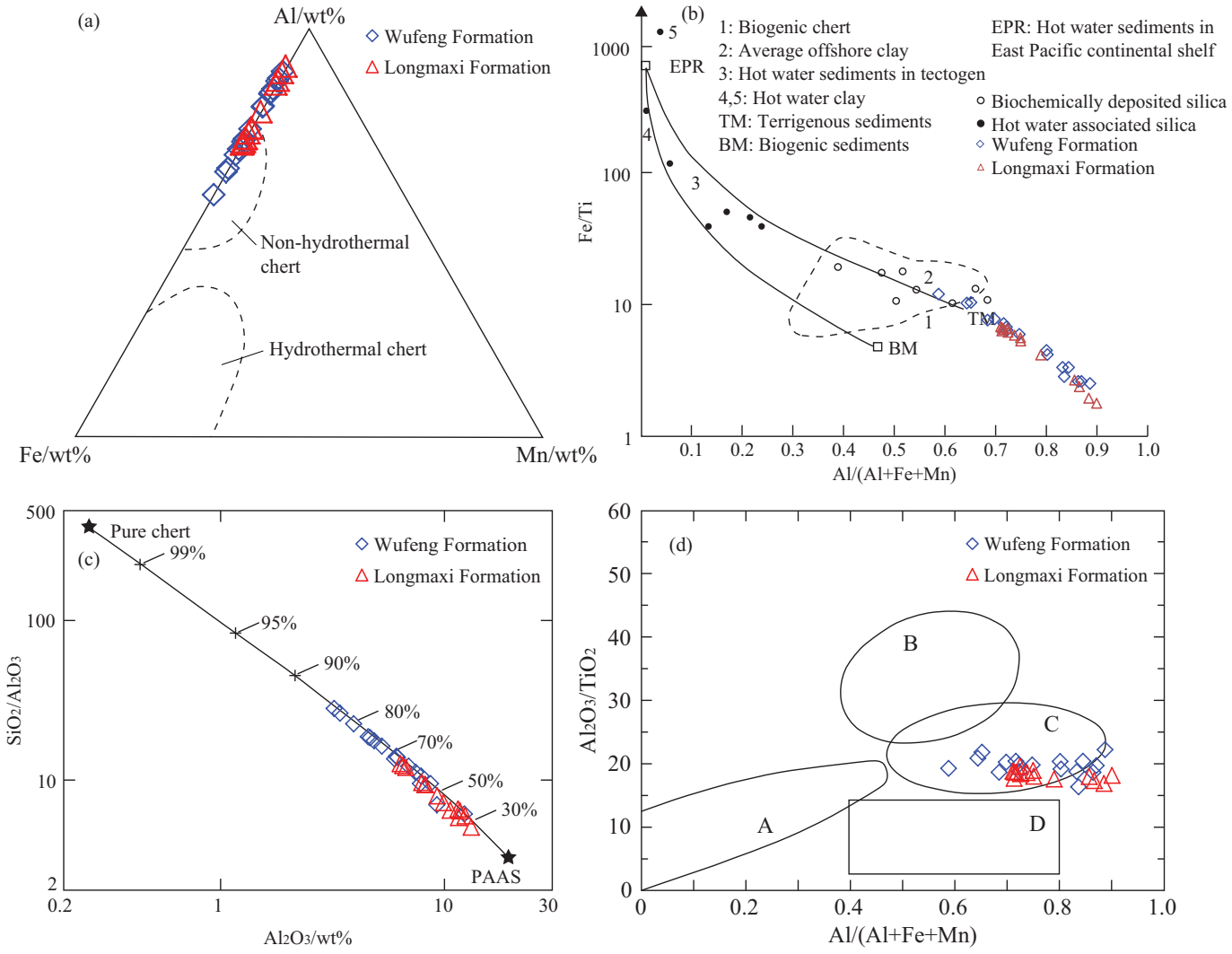

(Kunimaru et al. 1998; Kametaka et al. 2005). In our study, ∑REE of the bedded chert was up to 240.31 ppm and 322.92 ppm in the Wufeng and Longmaxi Formations, respectively. With a weak negative Eu anomaly and no notable Ce anomaly, the bedded chert in the Wufeng and Longmaxi Formations at the Qiliao section was therefore mainly influenced by terrigenous input rather than by hydrothermal fluid with light REE enrichment (Fig. 7).

5.1.2. Siliceous organisms: the key factor controlling the differences in the SiO_2 content

Excessive silica refers to SiO_2 content that is higher than that in the detrital sedimentary environment (Huang et al. 2012*b*; Wang et al. 2012). Wang et al. (2014) calculated excessive silica content when studying the siliceous origin of shale in the Wufeng and Longmaxi Formations at the Shuanghe section in the Sichuan Basin. Their results indicated that the SiO_2 content of shale in the Wufeng and Longmaxi Formations is up to 63% excluding the SiO_2 in the aluminosilicate. We observed that the excessive silica in the bedded chert ranged from 14.75% to 36.79% (average 28.18%) in the Wufeng Formation and from 9.35% to 27.0% (average 18.98%) in the Longmaxi Formation. Thus, the excessive silica of bedded chert in the Wufeng Formation was notably higher compared with the Longmaxi Formation. This phenomenon may be due to the excessive silica derived from siliceous organisms, which are notably higher in the bedded chert in the Wufeng Formation compared with the Longmaxi Formation.

In addition, volcanic activities during the Ordovician and Silurian transition had a global signature, and active volcanoes were present in the Sichuan Basin and its surroundings (Kolata et al. 1996; Bergström et al. 1995; Huff and Bergström 1995; Wang et al. 1983; Chen et al. 2000; Su et al. 2002, 2006; Lu et al. 2017). A large amount of volcanic ash layers were found in the siliceous strata in the Wufeng and Longmaxi Formations at the Qiliao section. Eight volcanic ash layers are present in the Wufeng Formation, which are thicker than those found in the Longmaxi Formation (Figs. 3 and 4). Meanwhile, thin section observations of the bedded chert indicate that more radiolarians, sponge spicules, and other siliceous organisms are present in the bedded chert in the Wufeng Formation compared with the Longmaxi Formation (Figs. 2–4). Furthermore, the volcanic ash, siliceous organisms, and SiO_2 content in the Wufeng Formation are all higher than those in the Longmaxi Formation. Many studies have reported that the abundance of nitrates, Fe, SiO_2, Mn, and other main and trace elements

Fig. 7. The rare earth element distribution patterns of bedded chert in the Wufeng and Longmaxi Formations at the Qiliao section (*a*) Wufeng Formation (WF) and (*b*) Longmaxi Formation (LMX). [Colour online.]

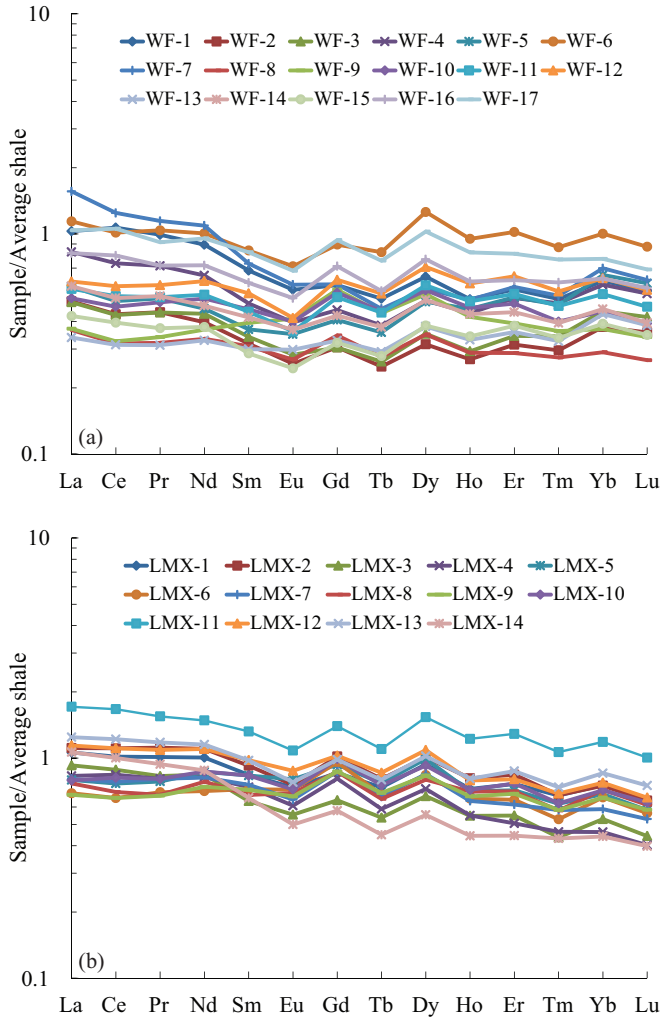

in volcanic ash could promote the growth of marine plankton and other marine organisms and improve marine primary productivity (Zhu et al. 1997; Frogner et al. 2001; Liu et al. 2005; Jones and Gislason 2008; Olgun et al. 2013). Therefore, a widespread volcanic ash input might have provided a source of silica and nutrients, which would result in the blooming of siliceous organisms and the higher SiO_2 content in the Wufeng Formation compared with the Longmaxi Formation.

To summarize, the origin of the bedded chert in the Wufeng and Longmaxi Formations at the Qiliao Section was interpreted to have been mainly influenced by terrigenous input and siliceous organisms rather than by hydrothermal fluid. Furthermore, volcanic activities played a significant role in the blooming of siliceous organisms, which was another key factor controlling the differences in the SiO_2 content in the bedded chert between the Wufeng and Longmaxi Formations.

5.2. Sedimentary environment of the bedded chert

The presence of major elements and REEs collectively indicates the sedimentary environment of chert. The ratio of $Al_2O_3/(Al_2O_3 + Fe_2O_3)$ could indicate the origin and sedimentary environment of chert, which ranged from 0.5 to 0.9 in the continental margin setting, less than 0.4 in the mid-oceanic ridge, and ranged from 0.4 to 0.7 in the ocean basin (Murray et al. 1991, Murray 1994). Some studies concluded that when the chert deposited near the continental margin, the ratio of $Al_2O_3/(Al_2O_3 + Fe_2O_3)$ was greater than 0.5 and the ratio of Fe_2O_3/TiO_2 was less than 50; when the chert deposited near the mid-oceanic ridge, the ratio of $Al_2O_3/(Al_2O_3 + Fe_2O_3)$ was less than 0.5 and the ratio of Fe_2O_3/TiO_2 was greater than 50 (Qiu and Wang 2010, 2011). Murray (1994) established some identification diagrams of sedimentary environment such as TFe_2O_3/TiO_2-$Al_2O_3/(Al_2O_3 + TFe_2O_3)$, $TFe_2O_3/(100\text{-}SiO_2)$-$Al_2O_3/(100\text{-}SiO_2)$, and $(La/Ce)_n$-$Al_2O_3/(Al_2O_3 + TFe_2O_3)$ based on the geochemical characteristics of the chert in different sedimentary environments from the Early Paleozoic to Tertiary era.

The ratios of $Al_2O_3/(Al_2O_3 + Fe_2O_3)$ of the bedded chert in the Wufeng Formation at the Qiliao section ranged from 0.65 to 0.91 (average 0.81), indicating deposition of the chert in the continental margin. Furthermore, the ratios of $Al_2O_3/(Al_2O_3 + Fe_2O_3)$ of the bedded chert in the Longmaxi Formation ranged from 0.76 to 0.92 (average 0.82), also suggesting formation in a continental margin setting. In addition, the ratios of Fe_2O_3/TiO_2 of the bedded chert in the Wufeng and Longmaxi Formations ranged from 2.2 to 10.2 (average 5.0) and 1.5 to 5.8 (average 4.2), respectively. The ratios of Fe_2O_3/TiO_2 of the bedded chert from both the Wufeng and Longmaxi Formations were less than 50, consistent with a continental margin setting. Based on the relationship diagram established by Murray (1994), most of the samples from the Wufeng and Longmaxi Formations at the Qiliao Section were evenly plotted in the continental margin field and were located far away from the mid-oceanic ridge (Figs. 8*a*, 8*b* and 8*c*).

Murray et al. (1991, 1992*a*, 1992*b*) and Murray (1994) found that in REEs in modern marine sediments, δCe generally increased with the increasing terrigenous input and varied from 0.18 to 0.6 (average 0.29) for the chert deposited near the mid-oceanic ridge, 0.5 to 0.76 (average 0.6) near the open ocean, and 0.67 to 1.52 (average 1.11) near the continental margin. In addition, from the mid-oceanic ridge to the open ocean basin to the continental margin, the $(La/Ce)_n$ of the chert decreased gradually. The $(La/Ce)_n$ of the chert deposited near the mid-oceanic ridge ranged from 1.66 to 5.19 (average 3.44), near the open ocean basin from 1.3 to 2.48 (average 1.82), and near the continental margin from 0.67 to 1.33 (average 0.93). However, the $(La/Yb)_n$ was opposite to the $(La/Ce)_n$. Influenced by terrigenous input, the $(La/Ce)_n$ would increase. The average $(La/Yb)_n$ of the chert deposited near the mid-oceanic ridge was about 0.3, about 0.7 for the chert deposited near the open ocean basin, and about 1.49 to 1.74 for the chert deposited near the continental margin.

The average δCe of the bedded chert in the Wufeng and Longmaxi Formations at the Qiliao Section were similar (average of 0.96 and 0.99, respectively). A continental margin setting is supported with the absence of obvious Ce anomaly in chert (average 1.11), which was similar to the chert of the continental margin in Francesco (1.02 ± 0.24) (Murray et al. 1991) and in ShooFly of America (1.05 ± 0.05) (Girty et al. 1996). $(La/Ce)_n$ of the bedded chert in the Wufeng and Longmaxi Formations was also similar with an average of 1.1 and 1.03, respectively, and were close to the chert formed in the continental margin setting (average 0.93). $(La/Yb)_n$ of the bedded chert in the Longmaxi Formation (average 1.43) was slightly higher than that in the Wufeng Formation (average 1.23), and both were close to the chert at the continental margin.

Results of the comprehensive analysis of the aforementioned evidence suggest that the bedded chert in the Wufeng and Longmaxi Formations deposited in the continental margin environment during the Ordovician and Silurian transition.

6. Conclusions

All pieces of evidence, including the relationship diagrams of major elements (SiO_2, TiO_2, Al_2O_3, and TFe_2O_3), Fe/Ti-Al/(Al + Fe + Mn), Al_2O_3/TiO_2-Al/(Al + Fe + Mn), and Al_2O_3-SiO_2/Al_2O_3; the Al–Fe–Mn ternary diagram; REEs; excessive silica; and thin section

Fig. 8. Relationship diagrams of bedded chert sedimentary environment in the Wufeng and Longmaxi Formations at the Qiliao section. [Colour online.]

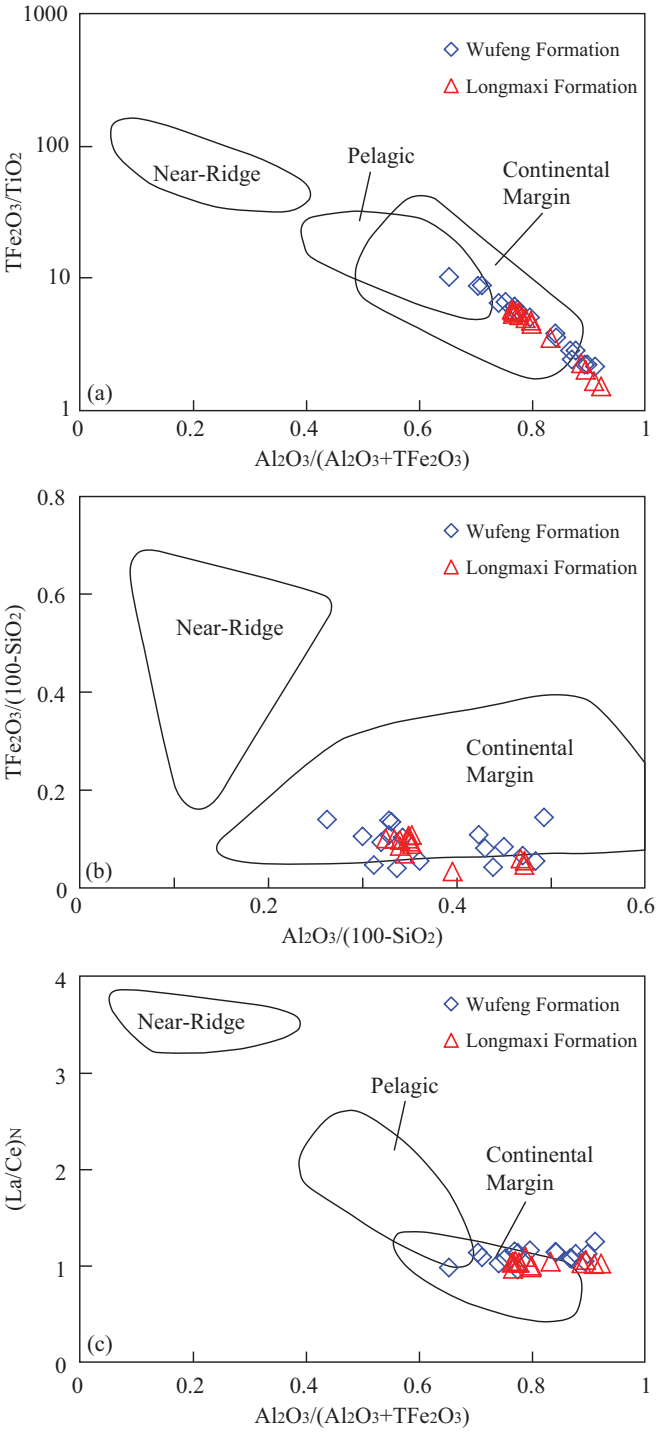

observation revealed that the origin of the bedded chert in the Wufeng and Longmaxi Formations at the Qiliao Section was influenced by terrigenous input and siliceous organisms as a normal marine chert and was slightly influenced by hydrothermal fluid.

Siliceous organisms were a key factor controlling the differences in the SiO_2 content of the bedded chert between the Wufeng and Longmaxi Formations at the Qiliao Section. In addition, volcanic ash, which could provide a source of silica and nutriment, played an important role in the blooming of siliceous organisms. Thus, volcanic activities were of great significance to the origin of the bedded chert in the Wufeng and Longmaxi Formations in the Shizhu area of Chongqing.

Geochemical indicators, such as TFe_2O_3/TiO_2-$Al_2O_3/(Al_2O_3 + TFe_2O_3)$, $TFe_2O_3/(100\text{-}SiO_2)$-$Al_2O_3/(100\text{-}SiO_2)$ and $(La/Ce)_n$-$Al_2O_3/(Al_2O_3 + TFe_2O_3)$; δCe; $(La/Ce)_n$; $(La/Yb)_n$ and other characteristic elements and ratios, indicated that the bedded chert in the Wufeng and Longmaxi Formations deposited in a continental margin environment during the Ordovician and Silurian transition.

Acknowledgements

This work was supported by the National Natural Science Foundation of China (grant numbers 41602119, 41690131, 41572327, and 41773056) and Scientific Research and Technological Development Program of CNPC (grant number 2016B-0302-01). We thank Jie Zhou, Zengguang Jiang, and Xin Tan for their assistance in the thin section observation and geochemical analyses. We also thank Dr. Xiqiang Zhou and Dr. Zhiyang Li for their constructive suggestions. We are grateful to two anonymous reviewers and the editor Dr. Hao Deng for helpful reviews.

References

Adachi, M., Yamamoto, K., and Sugisaki, R. 1986. Hydrothermal chert and associated siliceous rocks from the northern pacific their geological significance as indication of ocean ridge activity. Sedimentary Geology, **47**(1–2): 125–148. doi:10.1016/0037-0738(86)90075-8.

Bergström, S.M., Huff, W.D., Kolata, D.R., and Bauert, H. 1995. Nomenclature, straigraphy, chemical fingerprinting, and areal distribution of some Middle Ordovician K-bentonites in Baltoscandia. Geol Foeren Stockh Foerhand, **117**(1): 1–13. doi:10.1080/11035899509546191.

Bolhar, R., Kamber, B.S., Moorbath, S., Fedo, C.M., and Whitehouse, M.J. 2004. Characterisation of early Archaean chemical sediments by trace element signatures. Earth and Planetary Science Letters, **222**(1): 43–60. doi:10.1016/j.epsl.2004.02.016.

Boström, K., and Peterson, M.N.A. 1969. The origin of aluminum-poor ferromanganoan sediments in areas of high heat flow on the east pacific rise. Marine Geology, **7**(5): 427–447. doi:10.1016/0025-3227(69)90016-4.

Boström, K., Kraemer, T., and Gartner, S. 1973. Provenance and accumulation rates of opaline silica, Al, Ti, Fe, Mn, Cu, Ni and Co in Pacific pelagic sediments. Chemical Geology, **11**(2): 123–148. doi:10.1016/0009-2541(73)90049-1.

Chen, D.Z., Qing, H.R., Yan, X., and Li, H. 2006. Hydrothermal venting and basin evolution (Devonian, South China): constraints from rare earth element geochemistry of chert. Sedimentary Geology, **183**(3–4): 203–216. doi:10.1016/j.sedgeo.2005.09.020.

Chen, D.Z., Wang, J.G., Qing, H.R., Yan, D.T., and Li, R.W. 2009. Hydrothermal venting activities in the early Cambrian, South China: petrological, geochronological and stable isotopic constraints. Chemical Geology, **258**(3–4): 168–181. doi:10.1016/j.chemgeo.2008.10.016.

Chen, X., Rong, J.Y., Charles, E., Mitchell, David, A.T., Harper, Fan, J.X., Zhan, R.B., Zhang, Y.D., Li, R.Y., and Wang, Y. 2000. Late ordovician to earliest Silurian graptolite and brachiopod biozonation from the Yangtze Region, South China, with a global correlation. Geological Magazine, **137**(6): 623–650. doi:10.1017/S0016756800004702.

Dias, Á.S., Frühgreen, G.L., Bernasconi, S.M., and Barriga, F.J.A.S. 2011. Geochemistry and stable isotope constraints on high-temperature activity from sediment cores of the Saldanha hydrothermal field. Marine Geology, **279**(1–4): 128–140. doi:10.1016/j.margeo.2010.10.017.

Dong, D.Z., Gao, S.K., Huang, J.L., Guan, Q.Z., Wang, S.F., and Wang, Y.M. 2014. A discussion on the shale gas exploration & development prospect in the Sichuan Basin. Natural Gas Industry, **31**(12): 1–15. [In Chinese with English abstract.]

Douville, E., Bienvenu, P., Charlou, J.L., Donval, J.P., Fouquet, Y., Appriou, P., and Gamo, T. 1999. Yttrium and rare earth elements in fluids from various deep-sea hydrothermal systems. Geochimica et Cosmochimica Acta, **63**(5): 627–643. doi:10.1016/S0016-7037(99)00024-1.

Du, Y.S., Zhu, J., Gu, S.Z., Xu, Y.J., and Yang, J.H. 2006. Sedimentary geochemistry and tectonic significance of Ordovician cherts in Sunan, North Qilian Mountains. Earth Science-Journal of China University of Geosciences, **31**(1): 101–109. [In Chinese with English abstract.]

Du, Y.S., Zhu, J., and Gu, S.Z. 2007. Sedimentary geochemical characteristics of the Cambrian-Ordovician siliceous rocks and their implications for the Multi-Island in Sunan, North Qilian Mountains. Science in China (Series D), **37**(10): 1314–1329. [In Chinese with English abstract.]

Frogner, P., Reynir Gíslason, S., and Óskarsson, N. 2001. Fertilizing potential of volcanic ash in ocean surface water. Geology, **29**(6): 487–490. doi:10.1130/0091-7613(2001)029<0487:FPOVAI>2.0.CO;2.

Girty, G.H., Ridge, D.L., Knaack, C., Johnson, D., and Al-Riyami, R.K. 1996. Provenance and depositional setting of paleozoic chert and argillite, Sierra Ne-

vada, California. Journal of Sedimentary Research, **66**(1): 107–118. doi:10.1306/D42682CA-2B26-11D7-8648000102C1865D.

He, Y.Y., Niu, Z.J., Yang, W.Q., Song, F., Wang, X.D., and Jia, X.H. 2016. Geochemical features of middle-upper Ordovician cherts series in central-southern Hunan and their implications for basin evolution during Ordovician. Geology in China, **43**(3): 936–952. [In Chinese with English abstract.]

Huang, H., Du, Y.S., Yang, J.H., Tao, P., Huang, H.W., Huang, Z.Q., Xie, C.X., and Hu, L.S. 2012*a*. Geochemical features of siliceous sediments of the Shuicheng-Ziyun-Nandan rift basin in the late paleozoic and their tectonic implication. Acta Geologica Sinica, **86**(12): 1994–2010. [In Chinese with English abstract.]

Huang, H., Du, Y.S., Huang, Z.Q., Yang, J.H., and Huang, H.W. 2013. Geochemical characteristics of Late Paleozoic siliceous rocks in western Guangxi and its implications for tectonic evolution of Youjiang Basin. Science in China: Earth Science, **43**(2): 304–316. [In Chinese with English abstract.]

Huang, J.L., Zou, C.N., Li, J.Z., Dong, D.Z., Wang, S.J., Wang, S.Q., Wang, Y.M., and Li, D.H. 2012*b*. Shale gas accumulation conditions and favorable zones of Silurian Longmaxi Formation in south Sichuan Basin, China. Journal of China Coal Society, **37**(5): 782–787. [In Chinese with English abstract.]

Huang, Z.C., Huang, Z.J., and Chen, Z.N. 1991. Volcanic rock and radiolarian silicilith of Wufeng Formation in Lower Yangtze region. Acta Sedimentologica Sinica, **9**(2): 1–15. [In Chinese with English abstract.]

Huff, W.D., Bergström, S.M. 1995. Castlemainian K-bentonite beds in the Ningkuo Formation of the Jiangshan Province: the first Lower Ordovician K-bentonites found in China. Palaeoworld, **5**: 101–103.

Jones, M.T., and Gislason, S.R. 2008. Rapid releases of metal salts and nutrients following the deposition of volcanic ash into aqueous environments. Geochimica et Cosmochimica Acta, **72**(15): 3661–3680. doi:10.1016/j.gca.2008.05.030.

Kametaka, M., Takebe, M., Nagai, H., Zhu, S., and Takayanagi, Y. 2005. Sedimentary environments of the Middle Permian phosphorite–chert complex from the northeastern Yangtze platform, China; the Gufeng Formation: a continental shelf radiolarian chert. Sedimentary Geology, **174**(3): 197–222. doi:10.1016/j.sedgeo.2004.12.005.

Kolata, D.R., Huff, W.D., and Bergstöm, S.M. 1996. Ordovician K-bentonites of eastern North America. Special Paper of the Geological Society of America, **313**: 1–89. doi:10.1130/0-8137-2313-2.1.

Kunimaru, T., Shimizu, H., Takahashi, K., and Yabuki, S. 1998. Differences in geochemical features between Permian and Triassic cherts from the Southern Chichibu terrane, southwest Japan: REE abundances, major element compositions and Sr isotopic ratios. Sediment. Geol. **119**(3–4): 195–217. doi:10.1016/S0037-0738(98)00046-3.

Lei, B.J., Que, H.P., Hu, N., Niu, Z.J., and Wang, H. 2002. Geochemistry and sedimentary environments of the Palaeozoic siliceous rocks in western Hubei. Sedimentary Geology & Tethyan Geology, **22**(2): 70–79. [In Chinese with English abstract.]

Li, W.H. 1997. Petrological characteristics of radiolarian silicalite and its geological significance of Lower Silurian in the Hanzhong region. Acta Sedimentologica Sinica, **15**(3): 171–173. [In Chinese with English abstract.]

Lin, L.B., Chen, H.D., and Zhu, L.D. 2010. The origin and geochemical characteristics of Maokou Formation silicalites in the eastern Sichuan Basin. Acta Geologica Sinica, **84**(4): 500–507. [In Chinese with English abstract.]

Liu, C.Y., Zhang, Z.B., and Chen, X.R. 2005. The mutual effects of nitric oxide and iron on the growth of marine microalga. Acta Oceanologica Sinica, **27**(6): 123–130. [In Chinese with English abstract.]

Liu, W., Xu, X.S., Feng, X.T., and Sun, Y.Y. 2010. Radiolarian siliceous rocks and palaeoenvironmental reconstruction for the Upper Ordovician Wufeng Formation in the Middle-Upper Yangtze area. Sedimentary Geology & Tethyan Geology, **30**(3): 65–70. [In Chinese with English abstract.]

Lu, B., Qiu, Z., Zhou, J., Dong, D.Z., Wang, H.Y., Xue, H.Q., and Zhou, S.W. 2017. The characteristics and geological significance of the K-bentonite in Wufeng Formation and Longmaxi Formation in Sichuan Basin and its peripheral areas. Acta Geologica Sinica, **52**(1): 186–202. [In Chinese with English abstract.] doi:10.12017/dzkx.2017.012.

Ma, W.X., Liu, S.G., Chen, C.H., Huang, W.M., Zhang, C.J., and Song, G.Y. 2011. Geochemical characteristics of the siliceous rock in the Upper Sinian Denying Formation in the eastern Chongqing, China. Bulletin of Mineralogy Petrology & Geochemistry, **30**(2): 160–171. [In Chinese with English abstract.]

Michard, A. 1989. Rare earth element systematics in hydrothermal fluids. Geochimica et Cosmochimica Acta, **53**(3): 745–750. doi:10.1016/0016-7037(89)90017-3.

Mou, C.L., Zhou, K.K., Liang, W., and Ge, X.Y. 2011. Early Paleozoic sedimentary environment of hydrocarbon source rocks in the Middle-Upper Yangtze region and petroleum and gas exploration. Acta Geologica Sinica, **85**(4): 526–532. [In Chinese with English abstract.]

Murchey, B.L., and Jones, D.L. 1992. A mid-Permian chert event: widespread deposition of biogenic siliceous sediments in coastal, island arc and oceanic basins. Palaeogeography Palaeoclimatology Palaeoecology, **96**(1): 161–174. doi:10.1016/0031-0182(92)90066-E.

Murray, R.W. 1994. Chemical criteria to identify the depositional environment of chert: general principles and applications. Sedimentary Geology, **90**(3-4): 213–232. doi:10.1016/0037-0738(94)90039-6.

Murray, R.W., Ten Brink, M.R.B., Jones, D.L., Gerlach, D.C., and Russ, G.P., III 1990. Rare earth elements as indicators of different marine depositional environments in chert and shale. Geology, **18**(3): 268–271. doi:10.1130/0091-7613(1990)018<0268:REEAIO>2.3.CO;2.

Murray, R.W., Ten Brink, M.R.B., Gerlach, D.C., Russ, G.P., III, and Jones, D.L. 1991. Rare earth, major, and trace elements in chert from the Franciscan Complex and Monterey Group, California: assessing REE sources to fine-grained marine sediments. Geochimica Et Cosmochimica Acta, **55**(7): 1875–1895. doi:10.1016/0016-7037(91)90030-9.

Murray, R.W., Ten Brink, M.R.B., Gerlach, D.C., Russ, G.P., and Jones, D.L. 1992*a*. Interoceanic variation in the rare earth, major, and trace element depositional chemistry of chert: Perspectives gained from the DSDP and ODP record. Geochimica et Cosmochimica Acta, **56**(5): 1897–1913. doi:10.1016/0016-7037(92)90319-E.

Murray, R.W., Ten Brink, M.R.B., Gerlach, D.C., Russ, G.P., III, and Jones, D.L. 1992*b*. Rare earth, major, and trace element composition of Monterey and DSDP chert and associated host sediment: Assessing the influence of chemical fractionation during diagenesis. Geochimica et Cosmochimica Acta, **56**(7): 2657–2671. doi:10.1016/0016-7037(92)90351-I.

Olgun, N., Duggen, S., Andronico, D., Kutterolf, S., Croot, P.L., Giammanco, S., Censi, P., and Randazzo, L. 2013. Possible impacts of volcanic ash emissions of Mount Etna on the primary productivity in the oligotrophic Mediterranean Sea: Results from nutrient-release experiments in seawater. Marine Chemistry, **152**(2): 32–42. doi:10.1016/j.marchem.2013.04.004.

Qiu, Z., and Wang, Q.C. 2010. Geochemistry and sedimentary background of the Middle-Upper Permian cherts in the Xiang-Qian-Gui region. Acta Petrologica Sinica, **26**(12): 3612–3628. [In Chinese with English abstract.]

Qiu, Z., and Wang, Q.C. 2011. Geochemical evidence for submarine hydrothermal origin of the Middle-Upper Permian chert in Laibin of Guangxi, China. Science in China (Series D), **54**(7): 1011–1023. [In Chinese with English abstract.] doi:10.1007/s11430-011-4198-x.

Qiu, Z., Zou, C.N., Li, J.Z., Guo, Q.L., Wu, X.Z., and Hou, L.H. 2013. Unconventional petroleum resources assessment: progress and future prospects. Natural Gas Geoscience, **24**(2): 238–246. [In Chinese with English abstract.]

Qiu, Z., Dong, D.Z., Lu, B., Zhou, J., Shi, Z.S., Wang, H.Y., Lin, W., Zhang, C.C., and Liu, D.X. 2016. Discussion on the relationship between graptolite abundance and organic enrichment in shales from the Wufeng and Longmaxi Formation, South China. Acta Sedimentologica Sinica, **34**(6): 1011–1020. [In Chinese with English abstract.] doi:10.14027/j.cnki.cjxb.2016.06.001.

Qiu, Z., Jiang, Z.G., Dong, D.Z., Shi, Z.S., Lu, B., Tan, X., Zhou, J., Lei, D.F., Liang, P.P., and Wei, H.Y. 2017. Organic matter enrichment model of the shale in Wufeng-Longmachi Formation of Wuxi area. Journal of China University of Mining &Technology, **46**(5): 923–932. [In Chinese with English abstract.]

Qiu, Z., Zou, C.N., Li, X.Z., Wang, H., Dong, D., Lu, B., et al. 2018. Discussion on the contribution of graptolite to organic enrichment and reservoir of gas shale: a case study of the Wufeng-Longmaxi Formations in south China. Journal of Natural Gas Geoscience, **3**(3): 147–156. [In Chinese with English abstract.] doi:10.1016/j.jnggs.2018.07.001.

Ran, B., Liu, S.G., Jansa, L., Sun, W., Yang, D., Ye, Y.H., Wang, S.Y., Luo, C., Zhang, X., and Zhang, C.J. 2015. Origin of the Upper Ordovician–lower Silurian cherts of the Yangtze block, South China, and their palaeogeographic significance. Journal of Asian Earth Sciences, **108**: 1–17. doi:10.1016/j.jseaes.2015.04.007.

Rong, J.Y. 1984. Ecostratigraphic evidence of regression and influence of glaciation of Late Ordovician in the Upper Yangtze area. Journal of Stratigraphy, **8**: 9–20. [In Chinese with English abstract.]

Sholkovitz, E.R. 1988. Rare earth elements in the sediments of the North Atlantic Ocean, Amazon Delta, and East China Sea; reinterpretation of terrigenous input patterns to the oceans. American Journal of Science, **288**(3): 236–281. doi:10.2475/ajs.288.3.236.

Simonson, B.M., Maliva, R.G., and Knoll, A.H. 2005. Secular change in the precambrian silica cycle: insights from chert petrology. Geological Society of America Bulletin, **117**(7): 835. doi:10.1130/B25555.1.

Su, W.B., He, L.Q., Wang, Y.B., Gong, S.Y., and Zhou, H.Y. 2002. Redox sensitive trace elements as paleoenvironments proxies. Science in China (Series D), **32**(3): 207–219. [In Chinese with English abstract.]

Su, W.B., Wang, Y.B., and Gong, S.Y. 2006. A new Ordovician-Silurian boundary section in Guizhou, South China. Geoscience, **20**(3): 409–412. [In Chinese with English abstract.]

Su, W.B., Li, Z.M., Ettensohn, F.R., Johnson, M.E., Huff, W.D., Wang, W., Ma, C., Li, L., Zhang, L., and Zhao, H.J. 2007. Distribution of black shale in the Wufeng-Longmaxi formations (Ordovician-Silurian), South China: major controlling factors and implications. Earth Science, **32**(6): 819–827. [In Chinese with English abstract.]

Sugisaki, R., Yamamoto, K., and Adachi, M. 1982. Triassic bedded cherts in central Japan are not pelagic. Nature, **298**(5875): 644–647. doi:10.1038/298644a0.

Thurston, D.R. 1972. Studies on bedded cherts. Contributions to Mineralogy & Petrology, **36**(4): 329–334. doi:10.1007/BF00444339.

Torsvik, T.H., and Cocks, L.R.M. 2013. Chapter 2: New global palaeogeographical reconstructions for the Early Palaeozoic and their generation. Geological Society London, Memoirs, **38**(1): 5–24. doi:10.1144/M38.2.

Tréguer, P.J., and De la Rocha, C.L. 2013. The world ocean silica cycle. Ann Rev. Mar. Sci. **5**(5): 477–501. doi:10.1146/annurev-marine-121211-172346. PMID: 22809182.

Wang, S.F., Zou, C.N., Dong, D.Z., Wang, Y.M., Huang, J.L., and Guo, Z.J. 2014.

Biogenic silica of organic-rich shale in Sichuan Basin and its significance for shale gas. Acta Scientiarum Naturalium Universitatis Pekinensis, **50**(3): 476–486. [In Chinese with English abstract.] doi:10.13209/j.0479-8023.2014.079.

Wang, X.F., Zeng, Q.L., Zhou, T.M., Ni, S.Z., Xu, G.H., Sun, Q.Y., Li, Z.H., Xiang, L.W., and Lai, C.G. 1983. The fossil group at the early stage of Ordovician and the early Silurian in the eastern three gorges area and the boundary of the Ordovician and Silurian boundary. Chinese Academy of Geological Sciences, Yichang Institute of Geology and Mineral Resources, **6**: 95–182. [In Chinese with English abstract.]

Wang, Y.M., Dong, D.Z., Li, J.Z., Wang, S.J., Li, X.J., Wang, L., Chen, K.M., and Huang, J.L. 2012. Reservoir characteristics of shale gas in Longmaxi Formation of the Lower Silurian, southern Sichuan. Acta Petrolei Sinica, **33**(4): 551–561. [In Chinese with English abstract.]

Wang, Z.C., Zhao, W.Z., Zhang, L., and Wu, S.X. 2002. Tectonic sequence and gas exploration in Sichuan. Geological Publishing House, Beijing, pp. 95–182. [In Chinese.]

Xu, Y.T. 1996. The characteristics of genetical geochemistry of the cherts. Geotectonica et Metallogenia, **20**(1): 20–28. [In Chinese with English abstract.]

Yamamoto, K. 1987. Geochemical characteristics and depositional environments of cherts and associated rocks in the Franciscan and Shimanto Terranes. Sedimentary Geology, **52**(1): 65–108. doi:10.1016/0037-0738(87)90017-0.

Yamamoto, K., Nakamaru, K., and Adachi, M. 1997. Depositional environments of "accreted bedded cherts" in the Shimanto terrane, southwest Japan, on the basis of major and minor element compositions. Journal of Earth & Planetary Sciences Nagoya University, **44**: 1–19.

Yu, B.S., Dong, H.L., Chen, J.Q., Li, X.W., and Lin, C.S. 2004. Rare earth and trace element patterns in bedded- cherts from the bottom of the Lower Cambrian in the northern Tarim Basin, northwest China: implication for depositional environments. Acta Geologica Sinica, **22**(1): 59–66. [In Chinese with English abstract.]

Yu, W.H., Du, Y.S., Cawood, P.A., Xu, Y.J., and Yang, J.H. 2015. Detrital zircon evidence for the reactivation of an Early Paleozoic syn-orogenic basin along the North Gondwana margin in South China. Gondwana Research, **28**(2): 769–780. doi:10.1016/j.gr.2014.07.014.

Zhang, B.M., Chen, X.H., Wei, K., Zhou, P., and Zhang, M. 2014. Geochemical features of the Upper Ordovician cherts in Chongyi-Yongxin area, southern Jiangxi and their geological significance. Geological Science & Technology Information, **33**(5): 9–15. [In Chinese with English abstract.]

Zhou, Y.Z. 1990. On sedimentary geochemistry of siliceous rocks originated from thermal water in Nandan-Hechi Basin. Acta Sedimentologica Sinica, **8**(3): 75–83. [In Chinese with English abstract.]

Zhou, Y.Z., Chown, E.H., Guha, J., Lu, H.Z., and Tu, G.Z. 1994. Hydrothermal origin of Late Proterozoic bedded chert at Gusui, Guangdong, China: petrological and geochemical evidence. Sedimentology, **41**(3): 605–619. doi:10.1111/j.1365-3091.1994.tb02013.x.

Zhou, Y.Z., He, J.G., Yang, Z.J., Fu, W., Yang, X.Q., Zhang, C.B., and Yang, H.S. 2004. Hydrothermally sedimentary formations and related mineralization in south China. Earth Science Frontiers, **11**(2): 373–377. [In Chinese with English abstract.]

Zhu, M.Y., Mou, X.Y., and Li, R.X. 1997. The role of iron in primary productivity in the sea. Journal of Oceanography, **15**(3): 51–56. [In Chinese with English abstract.]

Zou, C.N., Dong, D.Z., Wang, S.J., Li, J.Z., Li, X.J., Wang, Y.M., Li, D.H., and Cheng, K.M. 2010. Geological characteristics and resource potential of shale gas in china. Petroleum Exploration & Development, **37**(6): 641–653. [In Chinese with English abstract.] doi:10.1016/S1876-3804(11)60001-3.

Zou, C.N., Dong, D.Z., Wang, Y.M., Li, X.J., Huang, J.L., Wang, S.F., Guan, Q.Z., Zhang, C.C., Wang, H.Y., Liu, H.L., Bai, W.H., Liang, F., Lin, W., Zhao, Q., Liu, D.X., Yang, Z., Liang, P.P., Sun, S.S., and Qiu, Z. 2015. Shale gas in China: characteristics, challenges and prospects (I). Petroleum Exploration and Development, **42**(6): 753–767. [In Chinese with English abstract.] doi:10.1016/S1876-3804(15)30072-0.

Zou, C.N., Qiu, Z., Poulton, S.W., Dong, D.Z., Wang, H.Y., Chen, D.Z., Lu, B., Shi, Z.S., and Tao, H.F. 2018. Ocean euxinia and climate change "double whammy" drove the Late Ordovician mass extinction. Geology, **46**(6): 535–538. doi:10.1130/G40121.1.